AIAA JOURNAL
Vol. 48, No. 10, October 2010

Simple Technique for Precise Measurement of Transmission Loss of Planar Sound Waves

Koichi Mori,* Yoshiki Murahashi,† Yutaka Koga,‡ and Yoshiaki Nakamura§
Nagoya University, Nagoya 464-8603, Japan
M. K. Ibrahim¶
Cairo University, Cairo 12613, Egypt
and
Takashi Takahashi**
Japan Aerospace Exploration Agency (JAXA), Tokyo 182-8522, Japan

DOI: 10.2514/1.J050404

A simple technique is proposed to measure the transmission loss through a panel of arbitrary size. The present technique uses two anechoic rooms to simulate the free acoustic field. Different from the conventional methods, the incident angle, the sound pressure distribution, and the spectral distribution of the incident sound waves can be changed arbitrarily. By the calibration experiments, the reasonable capabilities of the prototype facility are confirmed. In the experiment, a panel is installed in between two anechoic rooms. For the sake of simplicity, quasi-planar sound waves are provided in the sound-source room at uniform sound pressure over the panel. The intensity of the transmitted sound waves is measured in the receiving room. The modal analyses and the transmission loss measurements are completed for three different materials: aluminum, honeycomb sandwich, and carbon composite. The results are useful to verify the numerical analyses.

I. Introduction

SOUND transmission through a fuselage panel has been studied widely for aerospace applications [1–6]. For example, it is a critical issue to minimize the cabin noise when developing a new aircraft with a quiet and comfortable cabin. The noise is originated mostly from the engines, and it is transmitted through the fuselage sidewalls into the aircraft cabin. At a stage of the development of the aircraft, the soundproof performance of a part of the fuselage is tested in conventional techniques in which the sound waves are incident to the test panel from all directions. Here, it should be noted that in the actual flight conditions, different from the conventional testing conditions, the sound sources are not distributed uniformly around the cabin but localized near the engine. The sound waves are actually incident onto a panel at the particular angle, and the sound pressure distribution is not uniform over the panel. The influences of the incident angle and the sound pressure distribution on the sound transmission will possibly be significant when such anisotropic materials, as the carbon composites (C/Cs) and such complex-structured materials, as the honeycomb sandwich panels, are used. The experimental data including these influences are useful in designing the soundproof structures of the fuselage. The same holds true for satellite-carrying rockets. Acoustic noise from the rocket engines is considered one of the severe problems in launching. A payload inside of a faring may be damaged by the strong vibration and the acoustic noise [5–8]. The acoustic noise has been reduced by the elaborate designs of the fuselage structure. In addition, a number of auxiliary acoustic devices have been proposed to suppress the acoustic noise in a narrow band of frequencies [9,10]. Here, we have to be concerned about the spectral distribution of the noise. Intense sound waves, even at a narrow band of frequency, and those at a resonance peak can cause considerable damage to the structural or electrical parts of the payload. To warrant the soundproof performance of a part of the faring, it is necessary to simulate not only the space distribution but also the fine spectral distribution of the incident sound waves in the acoustic testing.

Highly accurate computation software is being developed to predict the sound field outside and inside of a vehicle [2,7,8,11]. Noise control schemes for aircraft and rockets will be designed in further detail on the basis of the reliable computational analyses. In the demonstration experiments to verify the computational analyses, the incident angle of the sound waves and the distribution of the sound pressure over the test panel must be specified precisely. The data averaged over each one-third-octave band are not appropriate. The fine spectral data of the transmission loss (TL) near the resonance peak are fruitful for the purpose of verification. This is because material property such as the structural damping is reflected clearly in the spectral shapes of the resonance peaks.

Three conditions must be satisfied, both in the acoustic testing to simulate the real flight conditions and in the precise experiments to verify the computational analyses:

1) The incident angle and the amplitude distribution of the sound waves are controllable and precisely identifiable.

2) The size of the test piece is not limited by the other factors. (The size is related to the resonance frequency of the vibration.)

3) Fine spectral data can be acquired. Unfortunately, these conditions are not satisfied simultaneously in the conventional techniques of the sound transmission measurement.

Sound transmission through a panel is evaluated by the TL that is defined as the fraction of the incident sound intensity that is transmitted through the panel [12]. TL of planar sound waves through a planar panel is estimated, in the first-order approximation, using the mass law that assumes the infinite extent of the panel. In this case, TL is simply formulated as

Received 26 December 2009; revision received 26 May 2010; accepted for publication 21 June 2010. Copyright © 2010 by the American Institute of Aeronautics and Astronautics, Inc. All rights reserved. Copies of this paper may be made for personal or internal use, on condition that the copier pay the $10.00 per-copy fee to the Copyright Clearance Center, Inc., 222 Rosewood Drive, Danvers, MA 01923; include the code 0001-1452/10 and $10.00 in correspondence with the CCC.

*Lecturer, Department of Aerospace Engineering, Furo-cho Chikusa-ku. Member AIAA.

†Graduate Student, Department of Aerospace Engineering, Furo-cho Chikusa-ku.

‡Graduate Student, Department of Aerospace Engineering, Furo-cho Chikusa-ku. Member AIAA.

§Professor, Department of Aerospace Engineering, Furo-cho Chikusa-ku. Member AIAA.

¶Associate Professor, Department of Aerospace Engineering. Member AIAA.

**Senior Chief Engineer, Aerospace Research and Development Directorate, 7-44-1, Jindaiji, Higashimachi, Chofu-shi. Member AIAA.

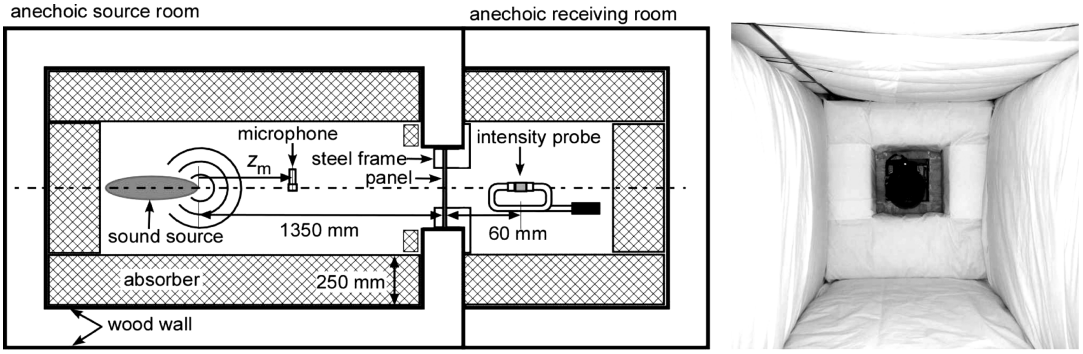

a) b)

Fig. 1 Experiment facility: a) schematic and b) source room (view from the window for test panel).

$$\mathrm{TL} = 20\log_{10}\left(\frac{2\pi f}{\rho_a c_a}\sigma\right) \tag{1}$$

where f is the frequency of the sound waves, ρ_a is the mass density of air, c_a is the sound speed of air, and σ is the surface density of the panel. According to the mass law, TL increases monotonously with the frequency, and its slope is determined by only one parameter (i.e., σ). For the actual panels of finite size, the spectra of TL are deviated from the mass law due to the resonance transmission generating spectral peaks. The central frequencies, the width, and the amplitude of the spectral peaks depends on the size, the material properties, the microscopic structure of the panel, and the incident angle of the sound waves [13]. To take the resonance transmission into account, the experimental testing is indispensable.

For the laboratory setup to measure TL, three different methods have been employed. The most conventional one is called the reverberant room method; two reverberant rooms, between which a test panel is installed, are employed. This method is stated, for example, in the International Organization for Standardization (ISO)/draft international standard (DIS) 140 [14]. As the sound field is diffused in a reverberant source room, the sound pressure is considered uniform over a panel surface, whereas sound waves come to the test panel randomly from all directions. The sound waves transmitted through the test panel are also diffused in the reverberant receiving room. The mean sound pressure is measured using microphones in both rooms. The second method is called the sound intensity method, where the receiving room is altered to an anechoic room [13]. Using an intensity probe, the distribution of the sound intensity of the transmitted sound waves is measured in the receiving room. Problems in using a reverberant source room are the space and spectral uniformity of the sound pressure and the incident angle of the sound waves. The distribution of the sound pressure over a panel is determined by the design of a reverberant room (i.e., wall materials, room shape, window shape (Niche effects), and the location of the loudspeaker). These many design parameters make it difficult to define the distribution of the sound pressure level (SPL) on the test panel precisely. For the incident angles, only the random incidence is available; that is, the incident angle of the sound waves is not controllable. To control it, special treatments of the testing facility are necessary. Grosveld [2] used a pneumatic horn to provide the best approximation to the normal sound incident condition. The experimental TL obtained by this method is compared with the computational results on the assumption of the normal incidence of the sound waves. From the comparisons, they concluded that the disagreement between the experimental and the computational TL should be partly due to the incident angle different from normal. For the spectral distribution of the incident sound waves, many spectral peaks are generated due to the cavity resonance in the reverberant room. When we study the fine spectra of the TL, uniform spectral distribution of the incident sound waves are rather favorable to suppress the errors in reducing the data. Hence, it is not straightforward to satisfy the conditions 1 and 3, noted previously, in these conventional experimental methods for the TL measurement. Specifically, the spectral nonuniformity is problematic when we examine the nonlinear interactions between the extremely intense sound waves and the panel vibration. This is important in simulating the intense acoustic noise in launching a rocket [7,8]. A tailored spectral distribution of the incident sound waves is indispensable, because the nonlinear interactions are strongly dependent on the spectra of the incident sound waves.

The third method for the TL measurement is the standing wave tube method [14,15]; a specimen is installed on the middle of a tube. A planar standing wave is generated from a speaker at one end of the tube, and is normally incident to the specimen. This method features a rather small testing kit. Unfortunately, the size of the specimen is dependent on the available frequencies of the incident sound wave in this method. Hence, the previously mentioned condition 2 is not satisfied in this method. When we study the resonance transmission, which depends on the size of the test panel, the size and the frequency of the incident sound waves have to be controlled independently.

For making the comparison between the numerical and the experimental results, in addition to the previously mentioned work by Grosveld [2], the numerical study for a honeycomb sandwich panel should be raised as a pioneering work [11]. Panels, such as a honeycomb sandwich panel that is routinely employed in the aerospace applications, have complicated structures inside of the skins. Theoretical [16,17] and numerical [11] studies are performed.

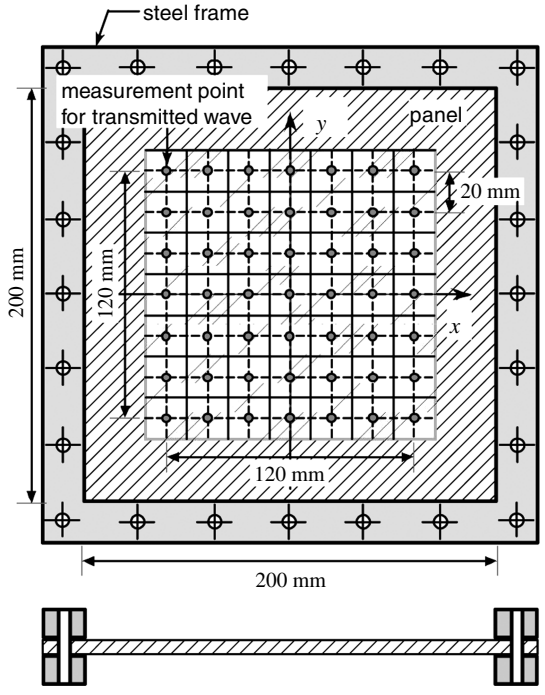

Fig. 2 Schematic of the fixing for the test panel and the matrix of the measurement points.

Table 1 Mechanical properties of the test panels

Properties	Aluminum (baseline)	Honeycomb	C/C 1 (quasi isotropic)	C/C 2 (unidirectional)	C/C 3 (unidirectional)
Thickness, mm	1.0	4.0	1.6	1.6	1.0
Surface density, kg/m^2	2.70	2.85	2.42	2.42	1.51
Young's modulus, GPa	69	17.25	54	141 (fiber)	76 (fiber)
Young's modulus, GPa	69	17.25	54	5 (lateral)	58 (lateral)
Shear modulus, GPa	26	——	——	7.1 (fiber)	——
Shear modulus, GPa	26	——	——	3.4 (lateral)	——

Table 2 Detailed specifications of the honeycomb panel

Parameter	Value
Surface thickness, δ, mm	0.5
Core height, h_c, mm	3.0
Core size, s, in.	3/16
Core foil thickness, in.	0.001
Compression strength, MPa	1.96
Shear strength, MPa	1.5 (L)
Shear strength, MPa	0.88 (W)

The theoretical model [16] agrees well with the spectral-averaged experimental data. The numerical results are compared with the fine spectral data acquired in the conventional setup [11]. They are in good agreement with each other in the qualitative sense. However, further investigations are still necessary, especially for the resonance peaks.

In the present paper, a simple but novel technique using two anechoic rooms is proposed for the measurement of TL. All the conditions from 1 to 3, noted previously, are satisfied simultaneously in the present technique. By using an anechoic room for the source room, the free acoustic field is simulated. The incident angle, the amplitude distribution, and the spectral distribution of the incident sound waves can be changed arbitrarily by the setup of the loudspeakers. Note that, unlike the standing wave tube methods, the panel size is not limited by the frequency range of interest. In the experiments, the TL data of a pure-aluminum panel, a honeycomb sandwich panel, and carbon-fiber reinforced plastics (CFRPs) are obtained. For the sake of simplicity, all the experiments are performed in the normal incidence of the sound waves at uniform sound pressure over the test panel. The characteristics of the resonance peaks are discussed. To the best of the authors' knowledge, the fine spectral data of these materials, including the resonance peaks, are obtained under the simple incident conditions of the sound waves here for the first time. The results are useful for the verifications of the following computational analyses.

II. Facility, Methods, and Materials

A. Facility

Figure 1 shows the schematic of the experiment facility. The facility consists of two anechoic rooms. The source room is designed to provide spatially uniform, temporally coherent, and planar sound waves normally incident onto the panel. The inner space is a box of $1640 \times 700 \times 700$ mm in the source room and $750 \times 700 \times 700$ mm in the receiving room. Layered acoustic absorbers are glued on the inner walls of these rooms. The absorber is 250 mm in thickness to absorb the sound waves for which the frequency is more than 200 Hz [18]. The absorber is made of triple layers of glass wool. The top layer has a thickness of 100 mm and a mass density of 12 kg/m^3, while those values are 50 mm and 20 kg/m^3 for the intermediate layer and 100 mm and 32 kg/m^3 for the bottom layer. The surface of the absorber is covered by a light fabric.

A loudspeaker (Omnisource loudspeaker 4295, Brüel and Kjær) is placed in the source room, as shown in Fig. 1a. Spherical sound waves are emitted from the head of the loudspeaker. The head is located 1350 mm away from the test panel surface. The axis of the loudspeaker is aligned along the center axis of the facility, which is normal to the test panel. The distance between the test panel and the loudspeaker is determined by the tradeoff between maximizing the planarity of the sound wave and maximizing the signal-to-noise ratio of the sound intensity measured in the receiving room. The exposed area of the test panel is a square with a side of 200 mm. The incident angle of the sound wave onto the panel is less than 6.0°. On the other hand, the SPL of the background noise is less than 20 dB within the frequency range of interest. The sound waves reached at the sidewalls of the source room are mostly absorbed.

The rigidly fixed panel is installed in between two anechoic rooms. A test panel is bound by two steel frames and is fixed using 24 bolts, as illustrated in Fig. 2. These bolts are clinched with a uniform torque by using a torque wrench, so that the four sides of the square panel are fixed rigidly and uniformly. Because the fixing affects the resonance of the panel vibration, TL is sensitive to the fixing condition.

B. Methods

The frequency of the sound waves from the loudspeaker is controlled using a function generator. The spectrum of the sound waves is kept uniform (white noise) in the frequency ranges from 200 to 2200 Hz. Note that the anechoic room is used for the source room. The cavity resonance due to reverberation in the room is never excited, and the spectra of the incident sound waves are uniform. Because the wave front of the incident waves is close to planar, the intensity of the incident waves can be approximated by the SPL [4]. The TL is calculated by subtracting the acoustic intensity level (IL) of the transmitted waves IL_t from the SPL of the incident waves SPL_i:

$$\mathrm{TL} = \mathrm{SPL}_i - \mathrm{IL}_t \tag{2}$$

SPL_i is measured using a microphone (4938, Brüel and Kjær) in the source room. The position of the microphone z_m, which is defined as the distance from the head of the loudspeaker along the axis, can be changed from 0 to 1 m. The time-series data of the sound pressure recorded using the microphone are converted to the spectrum series of SPL_i using a fast Fourier transform (FFT) analyzer (CF-521, Ono Sokki). IL_t is measured using an intensity probe (half-microphone pair 4197, dual preamplifier 2683, Brüel and Kjær). The intensity probe is located 60 mm away from the panel surface. The matrix of the measurement points are illustrated in Fig. 2. The IL is scanned over the panel within a 120×120 mm square. Each measurement

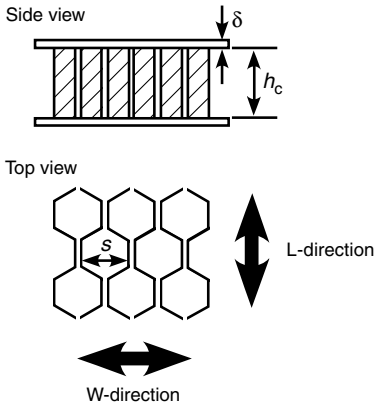

Fig. 3 Schematic of a honeycomb panel.

Table 3 Specification of the prepregs

Characteristics	Unidirectional prepreg A in C/C 1 and C/C 2	Unidirectional prepreg B in C/C 3	Plain-woven prepreg C in C/C 3
Young's modulus, E_a, GPa[a]	141	155	35
Young's modulus, E_b, GPa, [a]	5.0	8.96	35
Young's modulus, E_c, GPa[a]	5.0	8.96	10
Poisson ratio, ν_{ba}	0.011	0.02	0.3
Poisson ratio, ν_{ca}	0.011	0.02	0.085
Poisson ratio, ν_{ab}	0.3	0.3	0.085
Shear modulus, G_{ab}, GPa	7.1	7.1	7.1
Shear modulus, G_{bc}, GPa	3.4	3.4	7.1
Shear modulus, G_{ca}, GPa	7.1	7.1	7.1
Density, kg/m^3	1510	1497	1497

[a]Subscripts a, b, and c denote fiber direction, direction lateral to fiber, and thickness direction, respectively.

Table 4 ABD characteristics of the composite materials (without B matrix)

Panel	Matrix					
	A, N/m			D, N m		
C/C 1	9.60×10^7	2.60×10^7	0	34.8	4.61	2.23
	2.60×10^7	9.60×10^7	0	4.61	8.03	2.23
	0	0	3.50×10^7	2.23	2.23	6.52
C/C 2	2.31×10^8	2.41×10^6	0	49.3	0.514	0
	2.41×10^6	8.03×10^6	0	0.514	1.71	0
	0	0	1.14×10^7	0	0	2.42
C/C 3	9.59×10^7	6.74×10^6	0	4.24	0.813	0
	6.74×10^6	2.25×10^7	0	0.813	2.71	0
	0	0	7.10×10^6	0	0	0.592

point is separated 20 mm from the adjacent points. IL_t over the panel surface is evaluated by surface integrating the measured IL. TL data are presented in the spectral resolution of 8.0 Hz that is determined due to the performance of the FFT analyzer.

C. Materials

Three different kinds of materials are tested: pure aluminum, honeycomb sandwich, and CFRP. The mechanical properties of the tested panels are listed in Table 1. A pure-aluminum panel of 1 mm thick is selected as a baseline. The detailed specifications of the honeycomb panel are summarized in Table 2. The surface skins of the honeycomb sandwich panel are made of two pure-aluminum panels of 0.5 mm thick. The honeycomb core is made of thin foils of aluminum, as illustrated in Fig. 3, and its mass is negligible when compared with the skins. The mass in a unit area of the honeycomb panel is close to that of the baseline aluminum panel.

CFRP features the anisotropic nature of the elastic modulus. Three different CFRP panels, C/C 1, C/C 2, and C/C 3, are selected for the experiments. For all the CFRP panels, the hand layup method is used for the molding, and an autoclave is used for the hardening. The prepregs are made from epoxy resin and carbon fibers derived from polyacrylonitrile (Mitsubishi Plastics, Inc.). Three kinds of the prepregs, A, B, and C, are used. Their specifications are summarized in Table 3. The constitutive matrix is denoted as ABD. The ABD characteristics (ABD matrix) are listed in Table 4. All the components of the B matrix are zero for the materials used, and they are omitted in the list. The C/C 1 panel is a quasi-isotropic panel that is formed by laminating eight sheets of prepregs A. The fiber directions of the C/C 1 are depicted as $[0/45/-45/90/90/-45/45/0^\circ]$. The C/C 2 panel is a unidirectional panel formed by laminating the eight prepregs A in a single fiber direction. Both C/C 1 and C/C 2 panels have the same surface density and thickness. The surface density of these two panels is matched with the aluminum panel; however, the thickness is 1.6 mm larger than that of the aluminum panel. The C/C 3 panel is a unidirectional panel. The thickness of the C/C 3 is 1 mm and is the same as that of the aluminum panel. The C/C 3 panel is formed by laminating two different prepregs: B and C. Two sheets of the unidirectional prepregs B are sandwiched by two plain-woven prepregs C. The fiber directions of the two sheets of the prepregs B are same. Because the surface density of the aluminum, honeycomb sandwich, C/C 1, and C/C 2 are close to each other, the TLs of these panels are expected to be similar to each other on the basis of the mass law [Eq. (1)].

III. Calibration

The usage of anechoic source rooms is intended to simulate the three-dimensional free field, without any obstacles that cause the

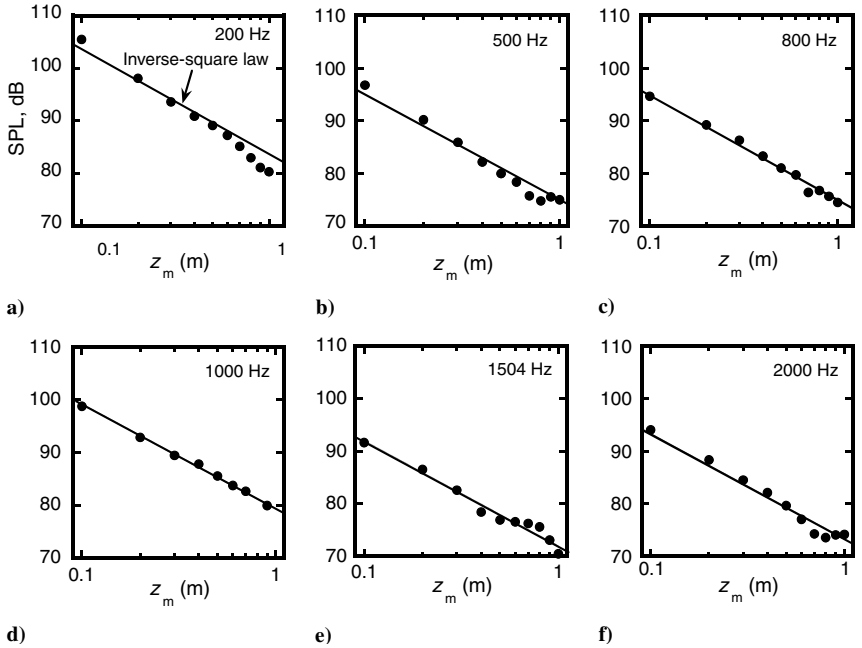

Fig. 4 Axial distribution of SPL in the anechoic sound-source room.

Table 5 Distribution of the relative deviation SPL (dB) on the panel surface at 1000 Hz

x, mm, y, mm	−50	0	50
−50	−0.21	0.12	0.25
0	−0.19	0.24	0.15
50	−0.24	−0.01	−0.11

reflection and diffraction of the sound waves. In the ideal free field, the sound waves emitted from a point source expand spherically. Their intensity decreases proportionally to z^{-2}, where z is the radial distance from the sound source in accordance with the so-called inverse-square law. On the other hand, the curvature of the wave front increases proportionally to z, and then the wave front becomes asymptotically planar. In the actual anechoic source room, the wall surface is covered by the absorber layers, except on a window for the test panel to simulate the three-dimensional free field. There are two factors to be considered. One is the reflection of the incident sound waves on the test panel. The other is the diffraction on the sidewalls. Even though the sound waves are absorbed by the absorber layers on the sidewalls of the room, the sound waves are diffracted due to the absorption. Both the reflection on the test panel and the diffraction on the sidewalls can cause perturbation onto the measurement of SPL_i. It is necessary to examine the sound pressure distribution in the actual anechoic source room.

To evaluate the deviation of the actual incident sound field from the inverse-square law, the longitudinal distribution of SPL was measured along the center axis in the source room. A microphone is traversed along the axis from 0.1 to 1.0 m away the speaker head. Monochromatic sound waves of a single frequency are emitted from the loudspeaker. The spectral frequency is ranged from 200 to 2000 Hz. The results are plotted in Figs. 4a–4f for the six different frequencies 200, 500, 800, 1000, 1504, and 2000 Hz, respectively. The closed circles represent the measured data, and the curves represent the inverse-square law. For all the tested frequencies, the measured results agree reasonably well with the theoretical values. The maximum discrepancy between the measured and the theoretical results is 3.5 dB at 200 Hz. It is 2.4 dB at 500 Hz, and it is less than 2.0 dB at the higher frequencies. It is natural that the difference, which is mainly originated from the reflection on the test panel, is significant near the test panel for all the frequencies. According to ISO 3745, the allowable differences between the inverse-square law and the measured SPL in the hemi-anechoic room are ±2.5 dB below the 630 Hz one-third-octave band, and ±2.0 dB for each of the one-third-octave bands between 630 and 6300 Hz [19]. The present facility satisfy this condition at the frequencies higher than 200 Hz. To reduce the errors, the incident SPL on the test panel, SPL_i, is extrapolated from SPL measured at the head of loudspeaker using a microphone on the basis of the inverse-square law.

The uniformity of SPL_i over the test panel is examined by measuring the cross-sectional distribution of SPL on a test panel. The SPL is measured at nine points in a 100 × 100 mm square around the center of the panel. To mount the microphones, a 20-mm-thick flat panel of aluminum is fixed on the window for the test panel. The microphones are flush mounted on the panel. The microphones and the panel are acoustically insulated from each other using a rubber tube. The relative SPL measured with a single frequency at 1000 Hz is shown in Table 5. The deviation of the SPL from the mean value is less than ±0.3 dB; uniform irradiation is realized. Figure 5 shows the spectral distribution of the maximum deviation of the SPL among the

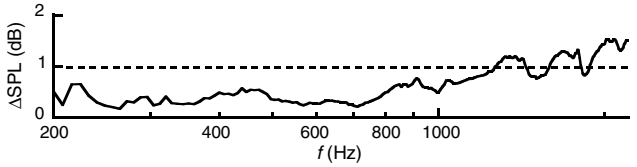

Fig. 5 Maximum deviation of SPL, ΔSPL, on the surface of the test panel.

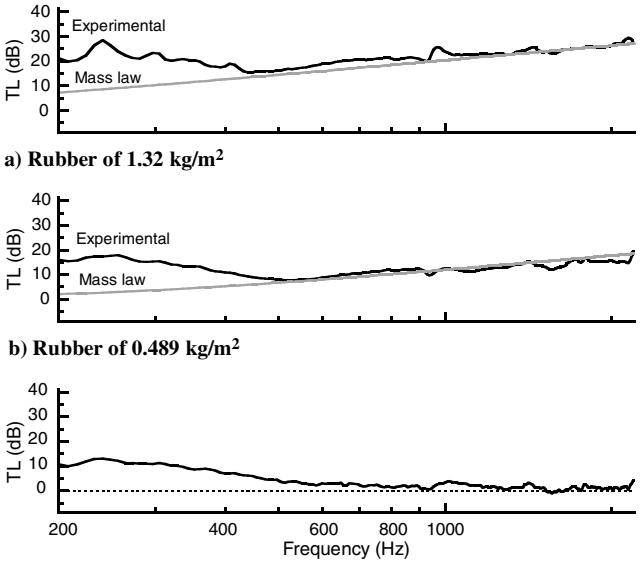

Fig. 6 TL through a rubber sheet.

measured nine point ΔSPL. In this case, white noise is used for the incident sound waves. In the frequency range from 200 to 1200 Hz, ΔSPL is kept around 0.5 dB at the frequencies lower than 800 Hz, and it then increases gradually with the frequency. The gradual increase in ΔSPL should result from the diffraction of the sound waves on the edge of the steel frame binding the test panel. Even at a higher frequency, ΔSPL is less than 2.0 dB.

Figure 6 shows the TL of a rubber sheet. Two rubber sheets, different in surface density, are tested. The TL for the thick rubber sheet, for which the surface density is 1.32 kg/m^2, is shown in Fig. 6a along with a theoretical curve of the mass law. The TL for the thin rubber sheet, for which the surface density is 0.489 kg/m^2, is shown in Fig. 6b. At the frequencies lower than 500 Hz, the experimental TL is higher than the theoretical. The difference between the experimental and the theoretical curves is around 14 dB at 200 Hz for both cases. It decreases with the frequency, and the two curves coalesce with each other at frequencies higher than 500 Hz. The standard deviation between the experimental and the theoretical TL is 0.77 dB for the thin rubber and 0.94 dB for the thick rubber in the range of frequencies from 500 to 2000 Hz. The TL is also measured with no panel installed in the window. The result is shown in Fig. 6c. The TL has a peak of 14 dB at 240 Hz, and it decreases with the frequency. In this case, two anechoic rooms and the aperture can be treated as a tube of the variable area, illustrated in Fig. 7. The TL is originated from the abrupt change in the cross-sectional area. The side length in the cross section of the anechoic room is 700 mm (see Fig. 1). This length, 700 mm, corresponds to the wavelength of the sound wave at the frequency of 491 Hz. At the frequencies lower than 491 Hz, the one-dimensional theory of the sound waves in pipes can be applied [20]. According to the theory, the TL is formulated as

$$\mathrm{TL} = 10\log_{10}\left[1+\frac{1}{4}\left(\frac{A_1}{A_2}-\frac{A_2}{A_1}\right)^2\sin^2\left(2\pi\frac{L}{\lambda}\right)\right] \qquad (3)$$

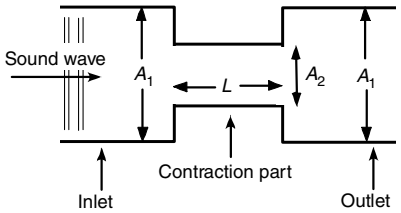

Fig. 7 Schematic of the sound transmission through a pipe of a variable cross-sectional area.

where the A_1, A_2, and L are the cross-sectional area in the inlet, the cross-sectional area of the contraction part, and the length of the contraction part, respectively, as illustrated in Fig. 7. The wavelength of the sound waves is λ. In the experiment, the side length of the square aperture is 200 mm, and then the ratio A_2/A_1 is 0.081. From Eq. (3), the maximum of the TL is calculated to be 16 dB, which is close to the measured maximum value, 14 dB. To be exact, the effects of the glass-wool absorbers should be taken into account. However, at the frequencies around 200 Hz, a large amount of the sound intensity is reflected on the wall, and the theory of the sound waves in a tube is valid. At the higher frequencies, the sound wavelength is smaller when compared with the size of the anechoic room, and the sound waves are mostly absorbed in the absorber on the wall of the anechoic room. As a result, the sound waves are transmitted perfectly through the aperture, as shown in Fig. 6c. By comparing Fig. 6c with Figs. 6a and 6b, the apparent excess of TL for the rubbers is presumably caused by the same reasons.

IV. Results

A. Aluminum Panel

The detailed spectrum of the TL for the aluminum panel is shown in Fig. 8a. The curve of the mass law, Eq. (1), is also drawn for comparison. Peaks that correspond to the resonance transmission appear clearly in Fig. 8a. The central frequencies of the peaks are 220, 830, 1360, and 1930 Hz.

Figure 8b shows the results of the modal analyses. The acceleration rate measured on the panel surface is plotted. For this result, the vibration is excited by an impact exerted on the panel. Several resonance peaks of the vibration are observed. To characterize the modal vibration, the resonance frequencies are computed using the commercial software LS-DYNA. Hexahedral mesh is used in the computations. The panel surface of a 200×200 mm square are split into 50×50 elements. For the boundary conditions, the translational and rotational motions of the nodes are constrained at the four sides of the square panel. The measured and computed resonant frequencies are listed in Table 6. The experimental and computed results agree reasonably well with each other within an error of 5.4%. In the experiment, the resonance frequency is sensitive to the fixing condition. This result ensures sufficient fixing rigidity of the test panel. Note that the several modes, like (1,2) and (2,1), are degenerated.

The modal shapes of the panel are illustrated in Fig. 9, where both points and solid lines represent the peaks of vibration, and the broken lines represent the nodes of vibration. A resonance peak is generated at the center of the square panel in the particular modes: the mode (1,1), the superimposed vibration of the degenerated modes (1,3) and (3,1) (depicted as $(1,3)+(3,1)$), the mode (3,3), and the superimposed $(1,5)+(5,1)$. Comparing Figs. 8a and 8b, it is clear that the peaks of the TL in Fig. 8a correspond to the particular resonant modes that have a peak of the vibration at the center of the panel. Such selective excitation of the modal vibration is originated from the uniformity of the SPL_i over the panel and the normal

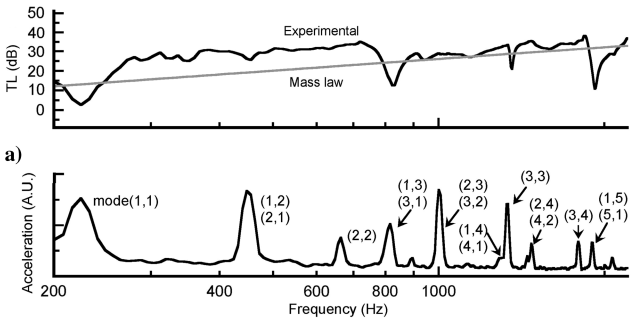

Fig. 8 TL and vibration of a pure-aluminum panel: a) TL and b) acceleration rate excited by the impact of a hammer.

Table 6 Resonant frequency of the aluminum panel (1 mm thick)

Mode	Computed (LS-DYNA), Hz	Measured, Hz	Difference, %
(1,1)	227	224	1.3
(1,2), (2,1)	463	448	3.2
(2,2)	684	664	2.9
(1,3), (3,1)	831	808	2.8
(2,3), (3,2)	1041	1000	3.9
(1,4), (4,1)	1335	1296	2.9
(3,3)	1388	1336	3.7
(2,4), (4,2)	1531	1448	5.4
(3,4)	1868	1792	4.1
(1,5), (5,1)	1962	1896	3.4

incidence angle of the sound waves. Otherwise, if the sound waves were obliquely incident on the test panel, different modes should have been excited. Hence, the present result ensures the uniform and normal incidence of the sound waves. At the frequency of the degenerated modes (1,2) and (2,1), a small dip appears in the TL curve in Fig. 8a. This may be originated from the small nonuniformity of the sound pressure and the incident angle different from normal.

Apart from the resonance transmission, in Fig. 8a, the experimental TL is higher than that of the mass law from 300 to 700 Hz, in between the first two peaks of TL. The experimental and the mass-law curves seem parallel to each other. The difference between two curves is constant at 10 ± 1 dB within this range of frequency. At the frequencies higher than the second peak of TL at 830 Hz, the experimental TL approaches the mass law, except at the peaks.

The width of the first peak of TL is around 30 Hz, and that of the second peak is 80 Hz. The shapes of these peaks are obtained in the resolution at 8 Hz, which is limited only by the capability of the FFT analyzer, and the data will be served for the verification of the numerical analyses.

B. Honeycomb Sandwich

The TL of the honeycomb sandwich panel is shown in Fig. 10a. At the frequencies lower than 500 Hz, the TL increases slightly with the frequency. The experimental TL curve seems parallel to that of the mass law. The difference between them is around 20 dB. It is higher than the aluminum by 10 dB. Unfortunately, the data are partly unavailable, because the transmitted IL is less than the background noise around 20 dB. At frequencies higher than 500 Hz, TL decreases monotonously with the frequency, up to the first peak at 930 Hz. The first peak of TL at 930 Hz corresponds to the first resonance frequency of the modal vibration shown in Fig. 10b. It should be noted that the peak of TL is not originated from the coincidence effects but from the resonance. When compared with the TL spectrum of aluminum (Fig. 8a), the first resonance frequency (930 Hz) is much higher than that of aluminum (220 Hz). At the resonance peak, TL is as low as 7 dB. Moreover, the width of the first peak of the honeycomb panel is larger than that of the aluminum. This is the case for both the TL and the modal vibration. The full width at half maximum of the first peak of the vibration is 130 Hz for the honeycomb panel, whereas it is around 30 Hz for the aluminum panel. The width of the first peak of TL of the honeycomb panel is around 300 Hz. From these results, it is clear that the resonance transmission is significant for the honeycomb sandwich panel rather than for the single leaf of the aluminum panel of the same surface density. However, it is not straightforward to explain the present trend. The aluminum panel (baseline) is equivalent to the sandwich panel of the zero core thickness. The resonant transmission is affected significantly by the core thickness, the bonding structure between the skins and the core, and the additional mass of the adhesive materials [16,17].

At the frequencies higher than 1000 Hz, the TL of the sandwich panel increases gradually with the frequency, then it gets close to the mass law, and it gets close to TL of the aluminum panel as well. The

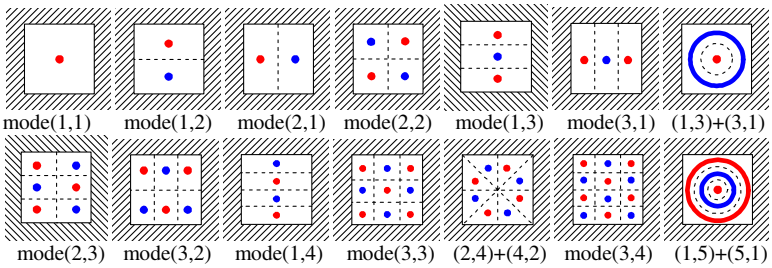

Fig. 9 Modal shapes of a square panel of isotropic material.

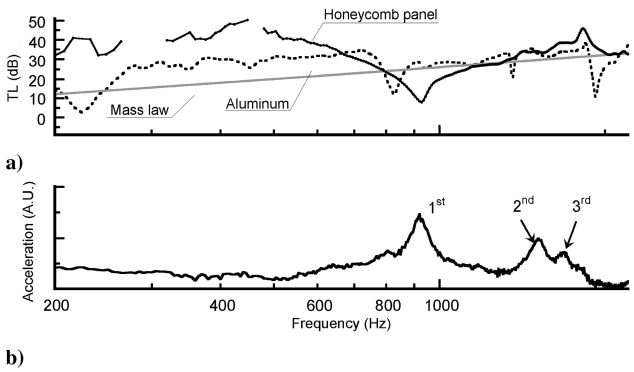

Fig. 10 TL and vibration of a honeycomb sandwich panel: a) TL and b) acceleration rate excited by an impact.

peak of TL does not appear at the frequencies corresponding to the second and third peaks of the modal vibration.

Detailed core structures including the adhesive materials have to be taken into account for the modal analyses of the honeycomb sandwich panels, as in the previous study [11]. It is above the scope of the present study and is left for future works. The detailed spectra of TL are sensitive to the core structure as well. The present measurement technique is useful to clarify the effects of the core structures on the sound transmission.

C. C/C Composite

Figure 11a shows the TL of the quasi-isotropic CFRP panel (C/C 1) and that of the unidirectional CFRP panel (C/C 2). The dark curve represents C/C 1, and the gray curve represents C/C 2. Because the surface density is the same with each, the curve of the corresponding mass law is common for both materials. Figures 11b and 11c show the acceleration excited by an impact of hammer. Although it is natural that the modal characteristics of the quasi-isotropic C/C 1 are similar to those of the aluminum panel, such modes as mode (1,2) and the mode (2,1) are not degenerated. In the spectrum of the TL, three peaks appear. These peaks correspond to modes (1,1), (1,3), and (3,1) of the resonance vibration. Figure 12 shows the maximum displacement of the surface of C/C 1 in the resonance vibration. This is computed using LS-DYNA. Because this quasi-isotropic panel is composed of eight sheets of the prepreg A, the panel is split into eight sheets in the thickness direction in the analysis. The specifications of the prepreg A, listed in Table 3, are employed in the analysis. The boundary conditions and the element numbers on the surface are the same as the analyses of the aluminum panel. As is apparent from Fig. 12, there is a peak of displacement at the center of the panel only in modes (1,1), (1,3), and (3,1). As is the case with the aluminum panel, resonance sound transmission occurs only at the particular resonance modes. Moreover, the antiresonance of the TL appears clearly in Fig. 11a at a frequency slightly lower than mode (1,3).

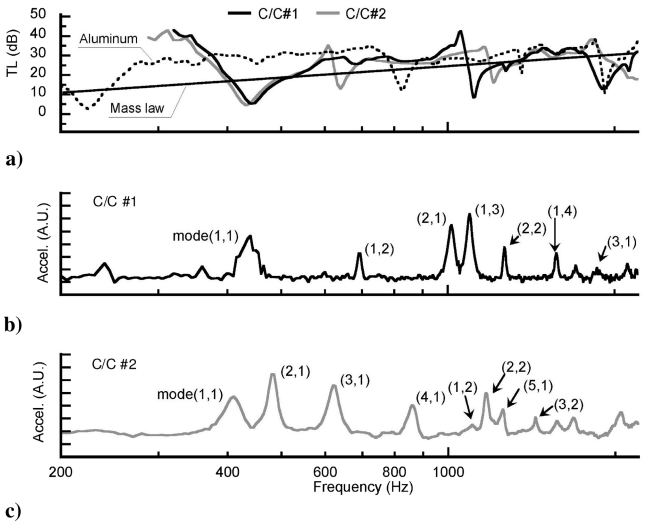

Fig. 11 TL and vibration of the quasi-isotropic CFRP panel (C/C 1) and the unidirectional CFRP panel (C/C 2): a) TL, b) acceleration rate of C/C 1 excited by an impact, and c) acceleration rate of C/C 2 excited by an impact.

For the C/C 2 panel, three peaks appear in Fig. 11a. The first peak of the TL is generated at a frequency in between the mode (1,1) and the mode (2,1), shown in Fig. 11c. In this case, the resonance frequencies of these two modes are extraordinarily close to each other (410 and 480 Hz). The peak of the TL is built up as a result of mutual interactions of these two modes of the vibration. The second and third peaks of the TL correspond to mode (3,1) and mode (5,1), respectively. Figure 13 illustrates the mode shapes in the resonance vibration of the C/C 2 panel. The same fact is repeatedly true in this case as well; that is, the TL has peaks at resonance modes (3,1) and (5,1), at which there is a peak at the center of the panel. Around the first peak of the TL, the TL curve of the C/C 1 and that of the C/C 2 are occasionally close to each other. The other resonance peaks of C/C 1 appear at frequencies different from the C/C 2. Apart from the resonance transmission, the TL gets close to the mass law as the frequency increases.

The TL spectrum of the C/C 3 is shown in Fig. 14a. The aluminum data are also plotted for comparison. Note that the C/C 3 and the aluminum are the same in thickness. In the figure, the relative TL that is defined as the measured TL subtracted by the theoretical value of the TL calculated from the mass law is presented. The frequency is normalized by the first resonant frequency f_{1st} of the TL of each material. Two curves, C/C 3 and aluminum, are occasionally very close to each other in the frequency range from the first peak to the second peak. This result seems interesting in a practical sense. Different from the resonance frequencies, it is not easy to predict the amplitude and the shapes of the peaks of the resonance transmission of the sound waves. On the basis of the fine spectral data, empirical scaling law may be formulated for the resonance sound transmission through C/C panels. Such a scaling law is useful in designing the

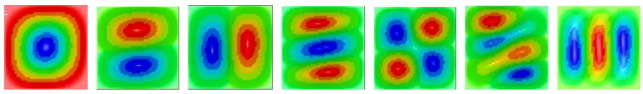

Fig. 12 Distribution of the maximum displacement in the resonance vibration of C/C 1 (calculated using LS-DYNA).

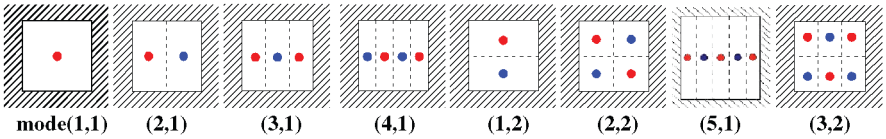

Fig. 13 Modal shapes of C/C 2.

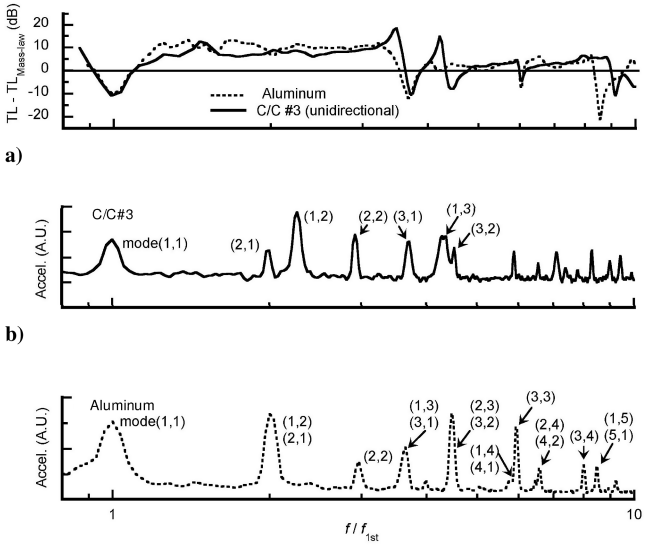

Fig. 14 TL and vibration of the unidirectional CFRP panel (C/C 3): a) TL, b) acceleration rate of C/C 3 excited by an impact, and c) acceleration rate of aluminum, presented for the comparison.

soundproof structures. To formulate the scaling law, a lot of experimental data of the resonance transmission are necessary.

Figures 14b and 14c show the spectra of the vibration. For the C/C 3, similar to C/C 2, the peaks of the TL correspond to modes (1,1), (1,3), and (3,1) of the resonance vibration. Needless to say, only in these modes, there is a peak at the center of the panel. Modes (1,3) and (3,1) are not degenerated. Because both the C/C 2 and C/C 3 are unidirectional, the modal shapes are similar, but the exact positions and shapes of the resonance peaks are different, depending on the material properties and thickness.

V. Conclusions

A simple anechoic room technique is developed to measure the fine spectra of the TL of sound waves through a panel. The incident angle, the distribution of the sound pressure, and the spectral distribution of the incident sound waves are arbitrarily controllable. Moreover, the shapes and the size of the test panel can be given arbitrarily. The present technique is successfully demonstrated in the measurement of the TL of a pure-aluminum panel, a honeycomb sandwich panel, and three different CFRP panels in the frequency range from 200 to 2000 Hz. For the sake of simplicity, the sound waves are incident in the direction perpendicular to the panel, and the SPL is kept uniform over the panel in the experiment. As a result, the resonance transmission of the sound waves occurs in the particular vibration modes, in which a peak of the oscillation appears at the center of the panel. This is true for the isotropic (aluminum), the quasi-isotropic (C/C 1), and the unidirectional materials (C/C 2). The experiment of the honeycomb sandwich panel revealed that the first resonance peak appears at a frequency higher than expected from the experimental results of the single leaf of aluminum of the same surface density. The width of the resonance peak of the honeycomb panel is much larger than the single leaf of aluminum. The results include the effect of the core and adhesive materials. For such panels of complex structure, as the honeycomb sandwich panels, the experimental data under the simplified conditions are useful to verify the numerical analyses.

Acknowledgments

The present study is completed as a part of the joint research between Nagoya University and the Japan Aerospace Exploration Agency (JAXA). The authors are grateful to the mutual discussions with T. Aoyama, K. Murakami, and A. Hashimoto, in the Computational Science Research Group in JAXA, and H. Kaneda, at the Research Center of Computational Mechanics, Inc.

References

[1] Vaicaitis, R., Grosveld, F. W., and Mixson, J. S., "Noise Transmission Through Aircraft Panels," *Journal of Aircraft*, Vol. 22, No. 4, April 1985, pp. 303–310. doi:10.2514/3.45124

[2] Grosveld, F. W., "Acoustic Transmissibility of Advanced Turboprop Aircraft Windows," *Journal of Aircraft*, Vol. 25, No. 10, 1988, pp. 942–947. doi:10.2514/3.45683

[3] Dowell, E. H., "Master Plan for Prediction of Vehicle Interior Noise," *AIAA Journal*, Vol. 18, No. 4, April 1980, pp. 353–366. doi:10.2514/3.50767

[4] Beyer, T. B., Powell, C. A., Daniels, E. F., and Pope, L. D., "Effects of Acoustic Treatment on the Interior Noise of a Twin-Engine Propeller Airplane," *Journal of Aircraft*, Vol. 22, No. 9, Sept. 1985, pp. 784–788. doi:10.2514/3.45202

[5] Lane, S. A., Kennedy, S., and Richard, R., "Noise Transmission Studies of an Advanced Grid-Stiffed Composite Faring," *Journal of Spacecraft and Rockets*, Vol. 44, No. 5, Sept.–Oct. 2007, pp. 1131–1139. doi:10.2514/1.28590

[6] Lane, S. A., Henderson, K., Williams, A., and Ardelean, E., "Chamber Core Structure for Faring Acoustic Mitigation," *Journal of Spacecraft and Rockets*, Vol. 44, No. 1, 2007, pp. 156–163. doi:10.2514/1.17673

[7] Murakami, K., Kitamura, K., Hashimoto, A., Aoyama, T., and Nakamura, Y., "Research on Acoustic Environment During Rocket Launch," *Theoretical and Applied Mechanics, Proceedings of the Japan National Congress for Applied Mechanics*, Vol. 56, 2008, pp. 463–470.

[8] Takahashi, T., Murakami, K., and Aoyama, T., "Steady-State Vibroacoustic Simulation for Launch Sites," *Theoretical and Applied Mechanics, Proceedings of the Japan National Congress for Applied Mechanics*, Vol. 57, No. , 2009, pp. 501–510.

[9] Grewal, A., Nitzsche, F., Zimcik, D. G., and Leigh, B., "Active Control of Aircraft Cabin Noise Using Collocated Structural Actuators and Sensors," *Journal of Aircraft*, Vol. 35, No. 2, March–April 1998, pp. 324–331. doi:10.2514/2.2303

[10] Zhao, L. J., Kim, H. S., and Kim, J., "Noise Reduction Using Smart Panel with Shunt Circuit," *AIAA Journal*, Vol. 45, No. 1, Jan. 2007, pp. 79–89. doi:10.2514/1.20077

[11] Grosveld, F. W., Buehrle, R. D., and Robinson, J. H., "Structural and Acoustic Numerical Modeling of a Curved Composite Honeycomb Panel," AIAA Paper 2001-2277, 2001.

[12] Fahy, F. J., *Foundations of Engineering Acoustics*, Academic Press, New York, 2001.

[13] Lee, J.-H., and Ih, J.-G., "Significance of Resonant Sound Transmission in Finite Single Partitions," *Journal of Sound and Vibration*, Vol. 277, Nos. 4–5, 2004, pp. 881–893. doi:10.1016/j.jsv.2003.09.023

[14] "Acoustics: Determination of Sound Absorption Coefficient and Impedance or Admittance by the Impedance Tube Method," International Org. for Standardization, ISO/DIS STD 10534, Geneva, 1994.

[15] Lee, C. M., and Xu, Y., "A Modified Transfer Matrix Method for Prediction of Transmission Loss of Multilayer Acoustic Materials," *Journal of Sound and Vibration*, Vol. 326, Nos. 1–2, 2009, pp. 290–301.
doi:10.1016/j.jsv.2009.04.037

[16] Dym, C. L., and Lang, D. C., "Transmission Loss of Damped Asymmetric Sandwich Panels with Orthotropic Cores," *Journal of Sound and Vibration*, Vol. 88, No. 3, 1983, pp. 299–319.
doi:10.1016/0022-460X(83)90690-9

[17] Nilsson, A. C., "Wave Propagation in and Sound Transmission Through Sandwich Plates," *Journal of Sound and Vibration*, Vol. 138, No. 1, 1990, pp. 73–94.
doi:10.1016/0022-460X(90)90705-5

[18] Beranek, L. L., and Sleeper, H. P., Jr., "The Design and Construction of Anechoic Chambers," *Journal of the Acoustical Society of America*, Vol. 18, No. 1, 1946, pp. 140–150.
doi:10.1121/1.1916351

[19] Grosveld, F. W., "Calibration of the Structural Acoustics Loads and Transmission Facility at NASA Langley Research Center," *Proceedings of Inter-Noise 99*, Inst. of Noise Control Engineering, Washington, D.C., Dec. 1999, pp. 1–6.

[20] Dowling, A. P., and Ffowcs Williams, J. E., *Sound and Sources of Sound*, Ellis Horwood, London, 1983, Chap. 3.

L. Cattafesta
Associate Editor